International Journal of Nanoelectronics and Materials

In Press, Accepted Manuscript – Note to user

Test Load Determination on Composite Standard Malaysian Rubber Constant Viscosity 60 for Earthquake Isolator

Mohd Azli Salim[1,2,*], Intan Raihan Asni Rosszainily[3], Adzni Md. Saad[1], Mohd Nizam Sudin[1] and Andrey N. Dmitriev[4]

[1]Fakulti Kejuruteraan Mekanikal, Universiti Teknikal Malaysia Melaka, Hang Tuah Jaya, 76100 Durian Tunggal, Melaka, Malaysia.
[2]Advanced Manufacturing Centre, Universiti Teknikal Malaysia Melaka, Hang Tuah Jaya, 76100 Durian Tunggal, Melaka, Malaysia.
[3]VisDynamics Research Sdn. Bhd, Lot 3844, Jalan TU 52, Kawasan Perindustrian Tasik Utama, Ayer Keroh, 75450 Melaka, Malaysia.
[4]Institute of Metallurgy of Ural Branch of Russin Academy of Sciences, 101, Amundsen st., Ekaterinburg, 620002, Russia.

ABSTRACT

This paper describes the test load determination on composite Standard Malaysia Rubber constant viscosity 60 for earthquake isolator. The usage of natural rubber in the development of earthquake isolator for building application has led to the investigation on its mechanical properties such as hardness, elastic modulus and many more. In this study, the mechanical properties of Standard Malaysian Rubber with constant viscosity 60 with various percentage of carbon black were investigated. The main purpose of this study is to implement the usage of Standard Malaysian Rubber as the main substance in the development of earthquake isolator. The nano-indentation was carried out by using Berkovich tips at a constant load with various holding time and it was recorded the highest hardness and elastic modulus values and also possessed then lowest penetration depth. This test also revealed that the hardness and penetration depth were independent of the holding time. In contrast, the indentation elastic modulus was found to be highly affected by the holding time. By using the nano-indentation test, it can determine the mechanical properties of Standard Malaysian Rubber, which is more cost-effective, non-destructive, and requires small test piece as compared to the conventional technique.

Keywords: composite Standard Malaysia Rubber, earthquake isolator, nano-identation.

1. INTRODUCTION

In general, there are two categories of rubber, which are known as natural and synthetic. Natural rubber (NR) is an organic material that is cultivated from the rubber tree by using tapping process. Tapping knife is used to shear the thin layer of rubber tree's bark in extracting the latex. The mostly used latex is harvested from Hevea Brasiliensis due to its superior quality, even though there are more than 2,500 plants that can produce latex. Contrarily, polymerization process of petroleum by-product is utilized to produce synthetic rubber. It is invented during World War 2 as a method of coping with the supply shortage of natural rubber. With the continuous development has been carried out, currently there are more than 20 types synthetic rubber has been produced and widely used. Due to its ability to be produced naturally, natural rubber can be introduced as green material. But, it possesses lower mechanical and chemical properties performance as compared to synthetic rubber. The cost of natural rubber is also more inexpensive and can be regularly supplied because it is produced using renewable sources [1]. On the other hand, the price of synthetic rubber is solely depended on the price of crude oil.

*azli@utem.edu.my

Natural rubber can be widely used in the application of reducing resonant effect. It is because, it has the capability of functioning as damper and spring-like performance. The strength of NR can also be increased by bonding it with other materials [3]. In addition, NR has the ability to instantly recover when distorted or deformed at room temperature by only permitting low heat to build up during in the applied dynamic force [2]. All these positive performances can be achieved by improving the properties of natural rubber using good formulation and processes.

The use of natural rubber, particularly in Malaysia is focusing on the engineering application as vibration isolator. Local fabricated dock fenders based on rubber are widely used as bumper in absorbing impact from collision between boat and jetty. The structure of Sultan Abdul Halim Muadzam Shah Bridge in Penang also uses 2234 high damping NR (HDNR) to absorb all the disturbances due to vibration influence. HDNR also has the well-known capability of withstanding large vibration originated from earthquake and other environmental perturbations.

The appeal of natural rubber in engineering applications is affected with the introduction of synthetic rubber. Even though the initial idea of using synthetic rubber is to reduce the reliance on natural rubber, but continuous improvement process has increased its performance especially in terms of resistance to oils, temperature and chemicals. Concurrently, natural rubber has also underwent various improvement processes. This NR can be processed with specific formulation, fillers addition and manufacturing method to meet specific requirements of the various engineering applications. The addition of fillers in natural rubber compound can highly affect the properties and strength of the compound. It is mainly depended on the filler type, size and loading. Unfortunately, the engineering applications of rubber in Malaysia are mostly relying on the imported material although locally manufactured rubbers show comparable performances.

On the other hand, based on previous research, it was found that the development of the vibration isolator for vibrating structure application is currently in trend [6-7]. Therefore, in this study, the application of Malaysian natural rubber, which is the vulcanized standard Malaysian rubber constant viscosity 60 (SMR CV 60) reinforced with carbon black as the potential main material is combined with the metal plate for the development of earthquake isolator has become the interest. This study focuses on the investigation of the vulcanized standard Malaysian rubber mechanical properties through the mechanical and nano-indentation testing. The objective of this study is to investigate the mechanical properties of standard Malaysian rubber that reinforced with different carbon loadings ranging from 0, 20, 40 and 60 phr through nano-identation test.

2. MATERIAL AND METHODS

The preliminary study regarding the transmissibility in the axial direction and parameter assessment on vibration isolator had been conducted in previous study [8]. Based on that, natural rubber shows promising potential to be utilized as the main material in the development of earthquake isolator. Further investigation is required particularly in terms of compatibility of using locally produced rubber grade as earthquake isolator. The purpose of this study is to evaluate the mechanical properties of rubber reinforced at various carbon loadings, which are at 0, 20, 40 and 60 phr. This section is describing the methodologies of preparing the material and nano-indentation test.

2.1 Sample Preparation

The natural rubber compound used in this study was named as the vulcanized SMR CV 60. By collaborating with Malaysian Rubber Board, the material preparation of milling, mixing, and the vulcanizing processes were prepared in the accreditation laboratory in order to maintain the quality of compounded rubber.

Complete formulation for the SMR CV 60 compound was tabulated in Table 1. The composition of ingredients for the rubber compound were prepared based on part per hundred of rubber (phr). The addition of sulfur helped to increase the crosslinking in rubbers, which resulting in the improvement of rubber texture from soft to hard. Meanwhile, the other ingredients such as zinc oxide, stearic acid, and CBS worked as the accelerator to boost up the sulfur crosslink efficiency. The N330 carbon black type was used as the filler since it was known as the most effective carbon in polymer reinforcement. Thus, in this study, the carbon loading in natural rubber compound was set as the changing parameter which varied at 0, 20, 40 and 60 phr. Besides that, the santoflex 13 and paraffin wax were also added into the compound as the ozone protective agent.

Table 1 Formulation for composite SMR CV 60

Ingredient	Amount (phr)
SMR CV-60	100
Zinc Oxide	5
Stearic Acid	2
CBS	0.8
Sulfur	3.25
Black HAF, N330	0, 20, 40, 60
Santoflex 13	3
Parafin Wax	2

ASTM D1382: Standard Practice for Rubber-Materials, Equipment, and Procedures for Mixing Standard Compound was used as the reference in determining all equipment specifications procedures of mixing and vulcanizing. As for the preparation of standard vulcanized rubber sheet, Preparing Standard Vulcanized Sheets was used as the guideline.

Dried natural rubber was blended with other ingredients in the rolling machine for 10 to 15 minutes as the initial step of compounding process. Then, this compound was allowed to reach its steady state by leaving it to rest for at least four hours. Next, it is proceeded with the vulcanization process, which can be referred as the treatment for rubber material in enhancing its elasticity and hardness by adding sulfur and an increased heat. This process is carried out for 8 to 12 minutes at the temperature of 150˚C. These parameters can be adjusted depending on the composition of carbon black in the natural rubber compound. The experimental specimens were produced in two different shapes. Cylinder with 6 mm height was produced for compression test and 2 mm rubber sheet for tensile test.

2.2 Nano-Indentation Testing Setup

The strength properties of material can be established by employing the indentation test on the surface of the material. For this specific study, Young's modulus and other properties can be obtained by using nano-indentation test including the effect of holding time on the material properties. The experimental works were carried by using the guidelines provided by E2546-15: Standard Practice for Instrumented Indentation Testing, which only provides the practical requirement of indentation test without specifying any test force, indentation depth range and specific type of indenter.

All tests were performed under the ambient temperature of 23 ˚C. The nano-indentation testing was conducted on eight samples with four different carbons loadings by using a nano-hardness tester. The nano-indenter device was equipped with an imaging device that capable to switch back and forth from the optical microscope to the indenter tips. The mounted imaging device

helps to identify accurately the desirable indentation point. A standard 115˚ triangular pyramidal indenter, the Berkovich type was used in this study.
For this testing purpose, the vulcanized natural rubber sheets specimens of 2 mm thickness were shaped into square pattern with the dimension of 10 mm x 10 mm. These test specimens' thickness must be at least 10 times of the maximum indentation depth (when conducting displacement assessment) or 6 times the indentation radius according to ASTM standard of E2546-15: the Standard Practice for Instrumented Indentation Testing. The size must also be adapted based on the indenter holder size. Prior of conducting the testing procedure, all the specimens must be wiped off with a damp cloth and let to be completely dried. It is because, the occurrence of dirt on the surface of the specimens can affect the indentation results.

During the process of conducting the nano-indentation test, the specimen must be kept stationary by mounting it on the platform. Then, the platform was moved to the indenter side after the indentation point was determined by placing it under the optical microscope. The load-hold-unload test with the fixed maximum test force of 2 mN and constant indenter loading speed of 0.2926 mN/sec was performed on 4 specimens with different carbon loadings. The determination of maximum test force value was determined in according to various test parameters such as the specimen's thickness, types of material, the probability of material to deform during indentation, surface finish and machine competency. In addition, the influence of holding time on indentation was also being investigated by varying the holding time of 0, 5, 10, 15 and 20 seconds. All the testing procedures were carried out with 3 repetitions, and the mean and standard deviation were calculated by using Equations 1 and 2.

$$\bar{x} = \frac{\sum fx}{n} \tag{1}$$

and

$$\bar{x} = \sqrt{\frac{\sum\left(x - \bar{x}\right)^2}{n-1}} \tag{2}$$

where $\bar{x}$ is the mean of values in the data set, n is the number of data set, and $\sum fx$ is the summation of the all data set. The s represent the standard deviation of the sample, $\sum$ means the "sum of", and x represent each value in the dataset.

This study was performed by experimentally neglecting sink-in and pile up effects. The recorded parameters were the maximum force (F_{max}), indentation depth (h_{max}), hardness (H_u) and Elastic Modulus (E_{it}).

3. RESULTS AND DISCUSSION

3.1 Bulk Resistivity of the Test Samples

This study provides the findings of conducting the nano-indentation test on vulcanized natural rubber compounds of SMR CV 60. An indentation-creep test was conducted at various holding times starting from 0 to 20 seconds. A fixed 2 mN test force was used as the maximum peak load. As there was no specific peak load stated in the ASTM standard, thus the peak load value was

determined by referring to previous studies as a precaution in order to avoid excessive applied force or the indenter tip to indent over the specimen.

Oyen in 2007 had determined the peak load level (P_{max}) range, depending on the materials Elastic modulus (Elastic) and Poisson's ratio (υ) [9]. This researcher applied P_{max} ranged from 1 mN and 10 mN to indent materials with E = 210 MPa and 4 MPa with the υ = 0.42 and 0.50, respectively. However, the researcher used a spherical tip to indent a 3.05 thick of material. Thus, by referring to the range of P_{max} as stated in previous research as the limit for maximum applied force and the Young's Modulus value obtained from the tensile and compression tests, the 2 mN test force was used in this study [10-11].

3.2 Effect of Carbon Black Loading

The experimental results for the nano-indentation test on SMR CV 60 filled with various carbon loadings of 0, 20, 40 and 60 phr were provided in Table 2. All values are in average. Based on the obtained results, the recorded maximum force ranged from 2.00 to 2.01 MPa in responds to the test constant parameter, which was the maximum indentation loads at 2mN. The relationship between maximum penetration depth, h_{max}, and the carbon loading of SMR CV 60 was presented in Figure 1. It was apparent from the figure that the h_{max} values were significantly decreasing with the increase of carbon loading. The h_{max} deviation values are 1, 0.25, 1, and 0.87 for 0, 20, 40 and 60 phr, respectively.

Table 2 The nano-indentation properties for composite SMR CV 60

Nano-indentation properties	Carbon loading (phr)			
	0	20	40	60
Maximum Force, F_{max} (mN)	2.01	2.01	2	2.01
Maximum depth, h_{max} (μm)	15.36	13.13	9.25	7.20
Hardness, H_u (MPa)	0.33	0.44	0.91	1.80
Elastic Modulus, E_{it} (MPa)	5.01	7.21	18.29	42.51

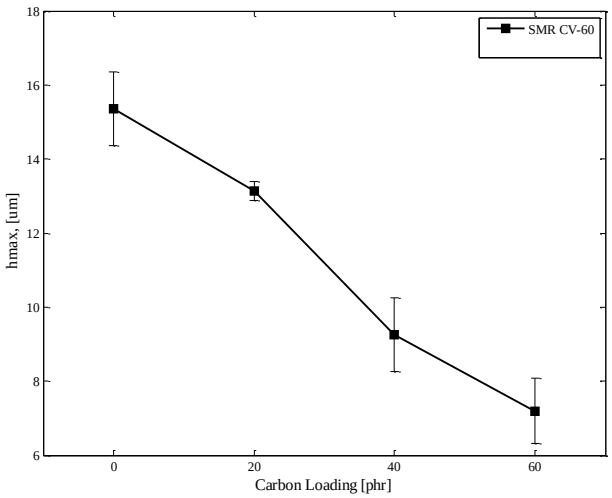

Figure 1. The graph of maximum indentation depth at different carbon loadings

Meanwhile the typical loading-unloading curves of force versus penetration depth at different carbon loadings were plotted separately in Figure 2. Based on the curve, it showed that the SMR CV with 60 phr was the hardest compound (right side). It was followed by the compound with 40 phr and 20 phr; while the softest is the SMR CV-60 with 0 phr. The viscous-elastic responses were

visible on each curve due to load-unload force [12]. The remnant depth at the end of the unloading curve showed the plastic deformation of the compound. It was randomly varied from 2.86 to 4.94 μm.

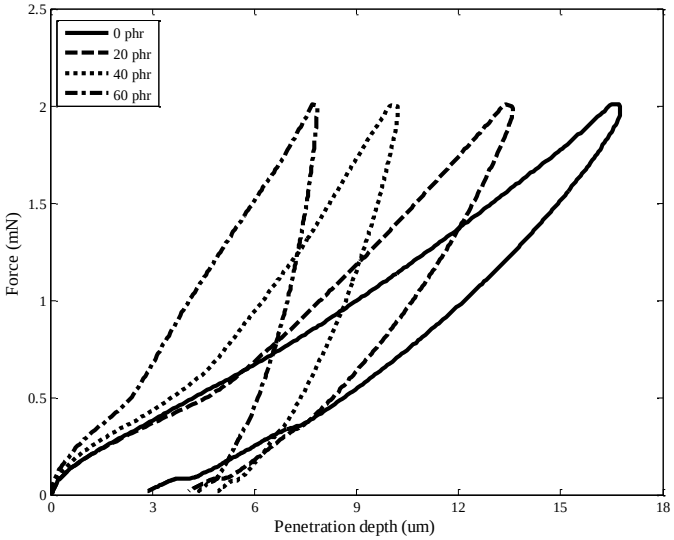

Figure 2. The nano-indentation loading-unloading curve at different carbon loading

As illustrated in Figure 1, the indentation depth increased as the carbon loading decreased, which was highly related to the compound hardness. The correlation between the compound hardness and carbon loadings for SMR CV 60 was presented in Figure 3. The hardness increased as the carbon content in the compounds was increased from 0, 20, 40, to 60 phr, respectively. Additionally, the graph also showed that the hardness value was proportional with the carbon loadings of 0 phr to 40 phr and achieved highest value at 60 phr. The hardness values at 0 phr was 0.33±0.04 MPa and it slightly increased at 20 phr with the value of 0.44±0.02 MPa. Then, at 40 phr, the hardness value was found to gradually increase with the value of 0.91±0.21 MPa. The hardness at 60 phr was 1.80±0.46 MPa. The increase of carbon black content in SMR CV-60 increased the stiffness, thus decreased the elasticity of the rubber. As the rubber becomes stiffer, it is harder for the indenter tips to penetrate into the rubber sample, which resulting of lower indentation depth as the compound contains high carbon loadings.

The graph of elastic modulus for the vulcanized SMR CV 60 at different carbon loadings under the indentation by using the Berkovich tip was depicted in Figure 4. Based on the figure, it was found that the elastic modulus for the SMR CV-60 was slightly increasing from 0 phr to 20 phr and significantly increasing for the carbon black content of 40 and 60 phr. As this study used Berkovich tips as indenter, the theories of Oliver and Pharr were applied to determine the elastic modulus. The E_{it} is equivalent to Young's modulus and can be calculated by rearranging the Equations (3) to (4).

$$\frac{1}{E_r} = \frac{1-\upsilon_s^{\,2}}{E_{it}} + \frac{1-\upsilon_i^{\,2}}{E_i} \tag{3}$$

$$E = \left(1-\upsilon_s^{\,2}\right)\left[\frac{1}{E_r} - \frac{1-\upsilon_i^{\,2}}{E_i}\right]^{-1} \tag{4}$$

where, E_r is the reduced elastic modulus that was determined through combination of material and indenter elastic deformation as in Equation 5, E_i and υ_i are Young's modulus and Poisson's

ratio of the indenter tips with the values of 1.14×10^{12} N/m^2 and 0.07, respectively. Then, υ_s is the Poisson's ratio of the specimen.

$$E_r = \frac{\sqrt{\pi}}{2\beta} \times \frac{S}{\sqrt{A_c}} \tag{5}$$

where β is the indenter constant, S is the stiffness at initial loading, and A_c is the area of contact surface.

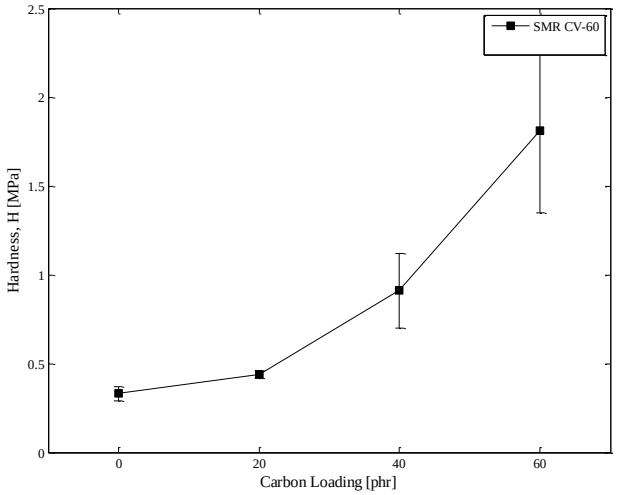

Figure 3. The graph of hardness versus the carbon loadings

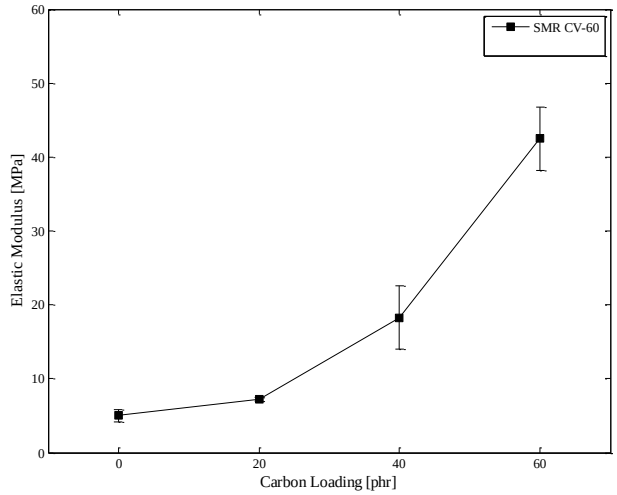

Figure 4. The graph of elastic modulus versus carbon loadings

3.3 Effect of Different Holding Times

This section discusses about the effect of different load holding times against the nano-indentation for Standard Malaysian Rubber. The experiment was conducted to investigate the nano-indentation at load holding times of 0, 5,10,15 and 20 seconds before the indenter tips was released. The results were illustrated as in Figure 5 below. The SMR allows the indenter tips to

reach maximum h_{max} at maximum loading force approximately from 11.15 s to 11.70 s. Then, the duration for the unloading is depended on the designated holding time.

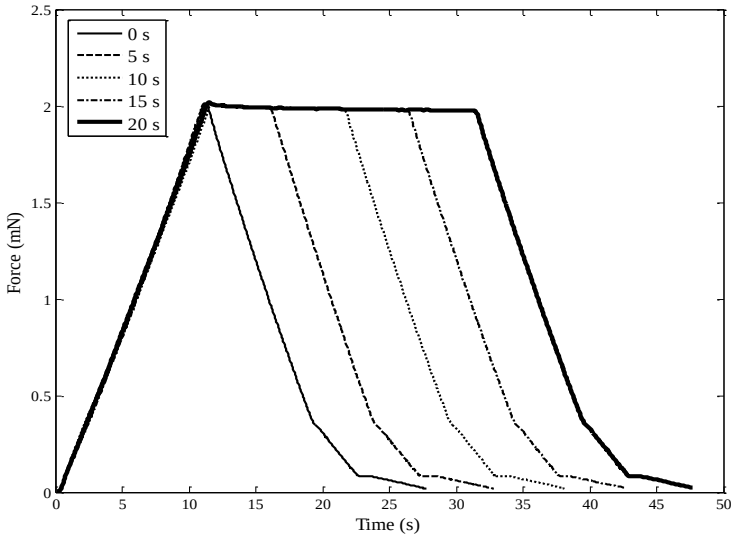

Figure 5. The graph of nano-indentation force versus holding time

The nano-indentation results for the SMR CV-60 was presented accordingly: Table 3 for holding time of 5 s, Table 4 for holding time of 10 s, Table 5 for holding time of 15 s, and lastly Table 6 for holding time of 20 s. Meanwhile, the nano-indentation result of 0 s holding time can be referred in previous Table 2.

Table 3 The nano-indentation properties at the holding time of 5 s

Nano-indentation properties	Carbon loading (phr)			
	0	20	40	60
Maximum Force, F_{max} (mN)	1.97	1.97	2.00	2.01
Maximum depth, h_{max} (μm)	16.55	13.65	10.08	6.22
Hardness, H_u (MPa)	0.28	0.41	0.78	2.36
Elastic Modulus, E_{it} (MPa)	4.15	6.87	14.55	45.47

Table 4 The nano-indentation properties at the holding time of 10 s

Nano-indentation properties	Carbon loading (phr)			
	0	20	40	60
Maximum Force, F_{max} (mN)	1.99	1.99	1.99	2.01
Maximum depth, h_{max} (μm)	18.14	13.30	9.85	6.68
Hardness, H_u (MPa)	0.23	0.43	0.88	1.71
Elastic Modulus, E_{it} (MPa)	3.61	7.85	16.15	48.93

Table 5 The nano-indentation properties at the holding time of 15 s

Nano-indentation properties	Carbon loading (phr)			
	0	20	40	60
Maximum Force, F_{max} (mN)	1.98	1.99	1.99	2.00
Maximum depth, h_{max} (μm)	19.28	13.50	10.10	5.34
Hardness, H_u (MPa)	0.20	0.42	0.80	2.23
Elastic Modulus, E_{it} (MPa)	3.09	7.90	15.12	56.16

Table 6 The nano-indentation properties at the holding time of 20 s

Nano-indentation properties	Carbon loading (phr)			
	0	20	40	60
Maximum Force, F_{max} (mN)	1.98	1.99	1.99	2.00
Maximum depth, h_{max} (μm)	18.90	12.47	9.15	6.13
Hardness, H_u (MPa)	0.21	0.49	1.02	2.06
Elastic Modulus, E_{it} (MPa)	3.21	9.08	18.17	55.21

The recorded E_{it} at different holding times was plotted in Figure 6. As shown in Figure 6, the E_{it} for the SMR CV-60 at 0 phr was found to decrease as the holding time increased, with the value from 5.01 MPa to 3.21 MPa. In contrast, with carbon loaded samples, the E_{it} value was found to increase with the increase of holding time. For 20 phr carbon, the E_{it} was slightly decreasing from 7.21 MPa to 6.87 MPa at 5s of holding time before it started to increase again. On the other hand, 40 phr and 60 phr showed a fluctuated trend for the E_{it} as the holding time increased. The E_{it} of 40 phr ranged from 14.55 MPa to 18.29 MPa. Meanwhile, the elastic modulus ranges for 60 phr was recorded from 42.51 MPa to 56.16 MPa.

As in nano-indentation, the holding time was applied to minimize the creep effect on the unloading curve, which may affect the modulus reading. In this study, it showed that the SMR CV 60 was slightly affected by the holding time where the E_{it} values varied with various holding times. In addition, by applying holding time before unloading can reduce the negative slope or the nose effect on the loading-unloading curve. The indentation curve for the SMR CV-60 compounds at various holding times was plotted and compared according to their carbon contents. The indentation curve for natural rubber at 0 phr carbons loading was presented in Figure 7. Meanwhile, the indentation curve at 20 phr and 40 phr of carbon loadings were presented in Figures 8 and Figure 9. Finally, the indentation curve at 60 phr of carbon was presented in Figure 10.

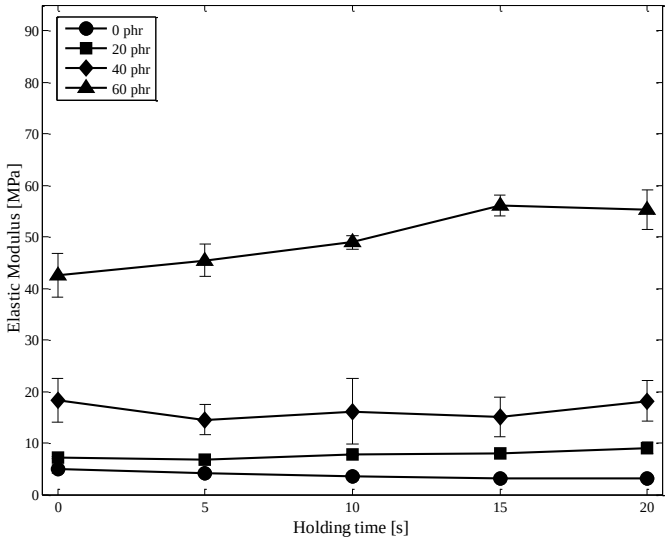

Figure 6. Graph of elastic modulus versus the holding time at different carbon loadings

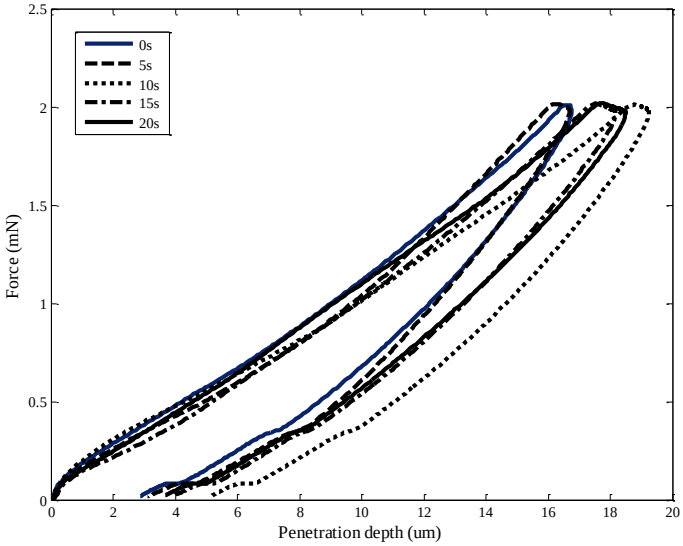

Figure 7. The graph of nano-indentation curve for 0 phr with various hold times

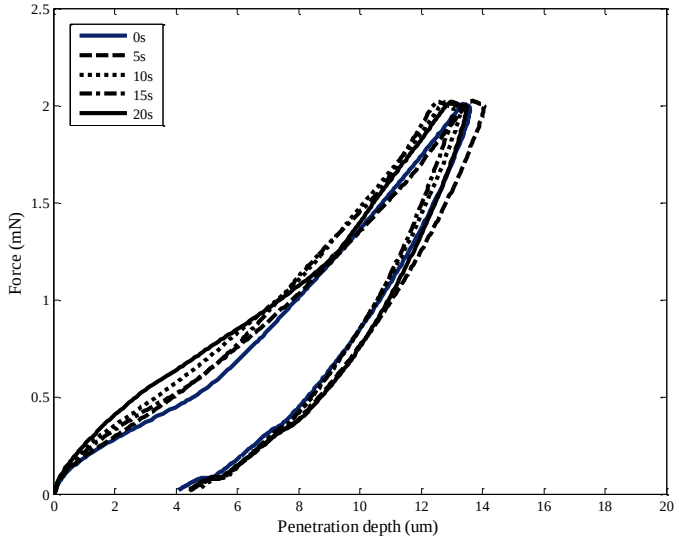

Figure 8. The graph of nano-indentation curve for 20 phr with various hold times

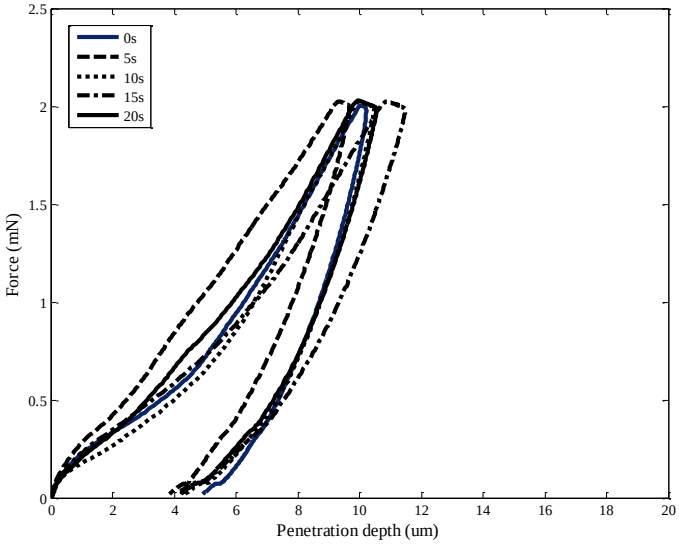

Figure 9. The graph of nano-indentation curve for 40 phr with various hold times

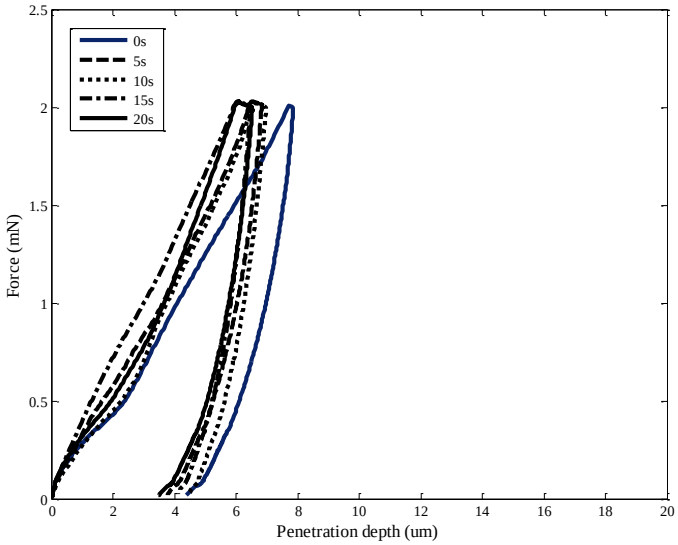

Figure 10. The graph of nano-indentation curve for 60 phr with various hold times

3.4 Nano-Indentation Work Dissipation

The results for the work dissipation, μ_{in} in the indentation of SMR CV 60 at different carbon loadings under different holding times were tabulated in Tables 7 and presented in Figure 11(a), (b), (c), & (d) based on their respective carbon loadings. It was apparent from these tables that the work dissipation values decreased as the carbon loading was increased. The dissipation of indentation work describes the corresponded mechanical work conducted through indentation and can be described as in Equation 6 below.

$$\mu_{in} = \frac{W_{in}^{elastic}}{W_{total}}(\%) \tag{6}$$

The μ_{in} is the parameter that refers to the ratio of indentation work value for the elastic component, $W_{in}^{elastic}$ to the total indentation work, W_{total}. The W_{total} is the total of elastic and inelastic work components, which is expressed as in Equation 7.

$$W_{total} = W_{in}^{elastic} + W_{in}^{inelastic} \tag{7}$$

Table 7 Work dissipation at different holding times

Work dissipation, μ_{in} (%)						
Carbon loading (phr)		**Holding time, (s)**				
		0	**5**	**10**	**15**	**20**
SMR CV 60	0	66.77	66.74	59.51	61.26	60.90
	20	58.48	54.78	49.32	47.35	47.29
	40	47.60	47.86	49.93	47.51	45.32
	60	34.98	31.99	28.27	27.64	34.32

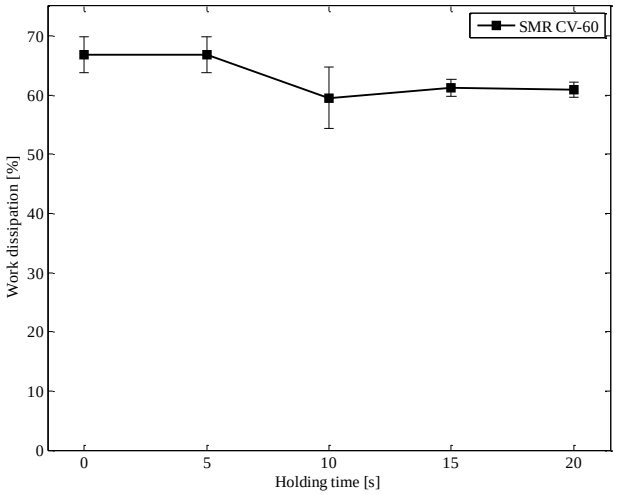

(a)

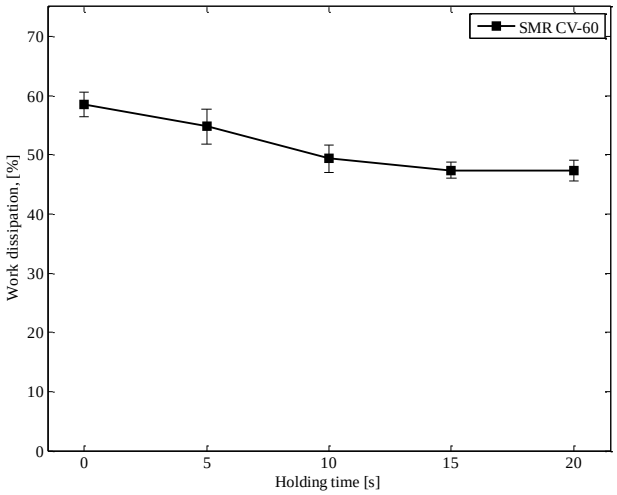

(b)

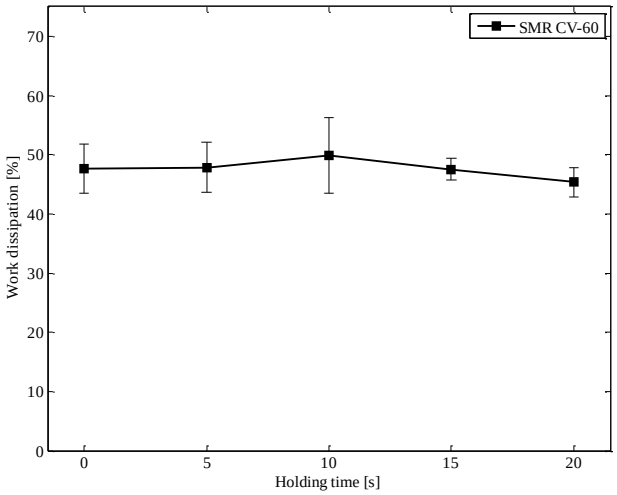

(c)

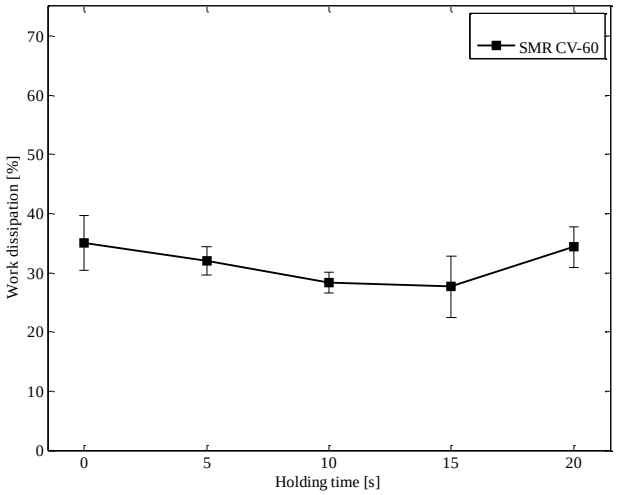

(d)

Figure 10. The graph of comparison for work dissipation versus holding time (a) 0 phr, (b) 20 phr, (c) 40 phr and (d) 60 phr

3.5 Correlation of the Results

The decreasing of penetration depth, h_{max} with the increasing of carbon black loading indented at constant 2 mN of maximum force showed that the properties of the vulcanized SMR CV 60 was influenced by the amount of carbon content. The influence of carbon content in natural rubber with the variation of viscous-elastic to elastic-plastic deformation modes could be observed in force-indentation depth curves. However, it is also showed that the remnant depth values were slightly depended on the carbon loading. This behavior was shown in the curve, where the remnant depth for unloading SMR CV 60 was lower than the carbon loaded while the remnant depth for unloaded [13].

The changes in h_{max} values at different carbon loadings in natural rubber also indicated the hardness of materials was increased as the carbon loading was increased too. However, in this study, the indentation size effect was neglected as there was no variation in test load values. The indentation size effect was referred to the increase of hardness with the decrease of indentation peak load [14]. Han et al., (2016) stated that the indentation side effect was not observed in some polymeric materials even though they were tested with pyramidal tip indenter [15].

On the other hand, according to Oliver and Pharr theory [16], the holding time could highly affect the elastic modulus for some material that indented by Berkovich tip [15]. Apparently as shown in this study, there have shown that the elastic modulus values were slightly depended on the holding time in the natural rubber at 0, 20 and 40 phr of carbon loadings. In contrast, significant changes were observed on 25 with high carbon content (60 phr) where the elastic modulus values were found to increase with the increasing holding time. Besides that, there were variations at the peak of force-penetration depth curve at different holding times. After all, this study also showed that the carbon loading was slightly depended on the indentation holding time.

The fluctuated values observed with lower carbon content were caused by the experimental uncertainties that affecting the nano-indentation test results such as machine compliance, thermal drift, and natural rubber surface roughness. The standard deviation bar showed in each graph represented the variation of values in collected data. Variation of collected data that was caused by the experimental uncertainties could directly affect the instrument performance and the indentation results. The instrument or machine compliance as calibration for initial contact

between the sample and mounted tips and imprecise machine stiffness value could significantly affect the measured nano-indentation force and penetration depth data. Besides that, the effect of thermal drift, which occurred due to the machine thermal expansion and heat generated by the continuously running electronic device was quite significant on the soft polymer, especially when indented at lower maximum depth and time relaxation [2, 17]. In addition, the surface roughness of the natural rubber did affect the measurement of mechanical properties.

Based on this study, it can be concluded that the nano-indentation technique can become an alternative to study the mechanical properties of material, especially in natural rubbers especially for earthquake isolator. By comparing to conventional test to study the mechanical properties of materials such as tensile and compression tests, the nano-indentation technique was non-destructive, cost effective and could be conducted in a smaller sample size. Atrian et al., in 2016 had conducted the tensile strength evaluation of Al7075-SiC nanocomposite by using spherical indentation test [18]. The results of this study agreed that the nano-indentation result was non-destructive, simple, cheaper and accurate as the actual tensile test. Due to the previous study, the nano-indentation data from this present study was found to satisfy the findings regarding the mechanical properties as compared to data obtained from conducted tensile and compressive tests.

4. CONCLUSION

The study was designed to determine the effect of carbon black loading on mechanical properties of natural rubber for vibrating structure like earthquake isolator. The mechanical properties of natural rubbers were determined in nano-indentation test. For the nanoscale test, a nano-indentation test was conducted by using the Berkovich tips indented with fixed force at 2mN with constant indenter loading speed of 0.2926 mN/sec. Besides that, the nano-indentation test was also conducted at various holding times of 0, 5, 10, 15, and 20 s to study the effect of holding time in order to determine the material properties. In this test, the maximum penetration depth, the hardness, and the elastic modulus were determined. Based on the obtained result, it can be concluded that the properties of natural rubbers were highly affected by the carbon loadings. The finding of this study is, the nano-indentation study also exhibited similar behavior as the other tests. The indentation properties improved with the increment of carbon loadings in terms of penetration depth, hardness, and elastic modulus. Meanwhile, in the investigation of the effect of holding time on the indentation of Berkovich tips, it showed that the indentation properties were independent of the holding time except for the elastic modulus properties. Last but not least, the design criteria for earthquake isolator can be designed by referring the mechanical properties data from this study.

ACKNOWLEDGEMENTS

Special thanks to Fakulti Kejuruteraan Mekanikal, Universiti Teknikal Malaysia Melaka (UTeM) for providing the laboratory facilities and financial supports under PJP/2016/FKM-CARE/S01506, PJP/2017/FKM/S01551 and PJP/2018/FKM(2B)/S01592.

REFERENCES

[1] Boonkerd, Kanoktip. Development and Modification of Natural Rubber for Advanced Application. Applied Environmental Materials Science for Sustainability. IGI Global (2017): 44-76.

[2] Chandrashekar, Gurudutt, Farid Alisafaei, and Chung-Souk Han. "Length scale dependent deformation in natural rubber." Journal of Applied Polymer Science 132, no. 43 (2015).

[3] Geethamma, V. G., G. Kalaprasad, Gabriël Groeninckx, and Sabu Thomas. "Dynamic mechanical behavior of short coir fiber reinforced natural rubber composites." Composites Part A: Applied Science and Manufacturing 36, no. 11 (2005): 1499-1506.

[4] Yu, Yunhe, Nagi G. Naganathan, and Rao V. Dukkipati. "A literature review of automotive vehicle engine mounting systems." Mechanism and machine theory 36, no. 1 (2001): 123-142.

[5] Kim, W. D., H. J. Lee, J. Y. Kim, and S-K. Koh. "Fatigue life estimation of an engine rubber mount." International Journal of Fatigue 26, no. 5 (2004): 553-560.

[6] Salim, Mohd Azli, Azma Putra, David Thompson, Nazirah Ahmad, and Mohd Azman Abdullah. "Transmissibility of a laminated rubber-metal spring: A preliminary study." In Applied Mechanics and Materials, vol. 393 (2013): 661-665. Trans Tech Publications.

[7] Salim, Mohd Azli, Azma Putra, and Mohd Azman Abdullah. "Analysis of axial vibration in the laminated rubber-metal spring." In Advanced Materials Research, vol. 845 (2014): 46-50. Trans Tech Publications.

[8] Salim, M. A., A. Putra, M. R. Mansor, M. T. Musthafah, M. Z. Akop, and M. A. Abdullah. "Analysis of Parameters Assessment on Laminated Rubber-Metal Spring for Structural Vibration." In IOP Conference Series: Materials Science and Engineering, vol. 114, no. 1 (2016): 012014. IOP Publishing.

[9] Oyen, Michelle L. "Sensitivity of polymer nanoindentation creep measurements to experimental variables." Acta Materialia 55, no. 11 (2007): 3633-3639.

[10] Medina, Nelson Flores, Darío Flores Medina, F. Hernández-Olivares, and M. A. Navacerrada. "Mechanical and thermal properties of concrete incorporating rubber and fibres from tyre recycling." Construction and building Materials 144 (2017): 563-573.

[11] Mazzotta, Francesco, Claudio Lantieri, Valeria Vignali, Andrea Simone, Giulio Dondi, and Cesare Sangiorgi. "Performance evaluation of recycled rubber waterproofing bituminous membranes for concrete bridge decks and other surfaces." Construction and Building Materials 136 (2017): 524-532.

[12] Oyen, Michelle L., and Robert F. Cook. "A practical guide for analysis of nanoindentation data." Journal of the mechanical behavior of biomedical materials 2, no. 4 (2009): 396-407.

[16] Callister, William D., and David G. Rethwisch. Materials science and engineering: an introduction. Vol. 7. New York: John wiley & sons, (2007).

[14] Xu, F., Y. H. Ding, X. H. Deng, P. Zhang, and Z. L. Long. "Indentation size effects in the nano- and micro-hardness of a Fe-based bulk metallic glass." Physica B: Condensed Matter 450 (2014): 84-89.

[15] Han, Chung-Souk, Seyed HR Sanei, and Farid Alisafaei. "On the origin of indentation size effects and depth dependent mechanical properties of elastic polymers." Journal of Polymer Engineering 36, no. 1 (2016): 103-111.

[16] Oliver, Warren Carl, and George Mathews Pharr. "An improved technique for determining hardness and elastic modulus using load and displacement sensing indentation experiments." Journal of materials research 7, no. 6 (1992): 1564-1583.

[17] Lin, D. C., E. K. Dimitriadis, and F. Horkay. "Elasticity of rubber-like materials measured by AFM nanoindentation." Express Polym Lett 1, no. 9 (2007): 576-584.

[18] Atrian, A., G. H. Majzoobi, S. H. Nourbakhsh, S. A. Galehdari, and R. Masoudi Nejad. "Evaluation of tensile strength of Al7075-SiC nanocomposite compacted by gas gun using spherical indentation test and neural networks." Advanced Powder Technology 27, no. 4 (2016): 1821-1827.